RESEARCH PAPER

Computational Study of the Anti-cancer Peptide VLL-28 Targeting Cathepsin L to Combat Epithelial Ovarian Cancer

Annu Choudhary[1], Nilima Kumari[2], Pushpender Kumar Sharma[1], Sandeep Kumar Shrivastava[3], Ravi Ranjan Kumar Niraj[1*] and Vinay Sharma[1*]

[1]*Amity Institute of Biotechnology, Amity University Rajasthan, Jaipur, Rajasthan, India*
[2]*Department of Bioscience & Biotechnology, Banasthali Vidyapith, Tonk, India*
[3]*Centre for Innovation, Research & Development (CIRD), Dr. B. Lal Clinical Laboratory Pvt.Ltd., India*
[*] ***Corresponding Authors:*** *Prof. (Dr).Vinay Sharma and Dr. Ravi Ranjan Kumar Niraj*
Amity Institute of Biotechnology, Amity University Rajasthan, Jaipur, Rajasthan, India
vinaysharma30@yahoo.co.uk and rrkniraj@gmail.com

Received: 28th Feb, 2026; Revised: 6th March 2026; Accepted: 7th April, 2026; Available Online: 20th April, 2026

ABSTRACT

Introduction: Ovarian cancer, the deadliest kind of gynecological malignancy, is a significant public health issue despite its uncommon occurrence. The World Health Organisation estimates that ovarian cancer will be diagnosed in 225,500 cases per year and that 140,200 individuals will die from the disease. This makes ovarian cancer the seventh most prevalent kind of cancer and the eighth most common cause of cancer-related death for women globally When combined, these numbers highlight the importance of ovarian cancer as a cause of illness and death for people worldwide. Ovarian cancer ranks fifth among women in Western countries who die from cancer. In this study. One cysteine protease that may be used as a therapeutic target in cancer treatment is cathepsin L. Inhibiting the activity of specific proteases can slow cancer progression. Peptide therapeutics are good as far as effectiveness and side effects are concerned.

Methods: In our study, we selected 274 anticancer peptides from databases and screened them against CatL as the target protein of EOC using the HDOCK server and then selected VLL-28 after analyzing various parameters. To validate the interaction of VLL-28 with CatL, we performed a molecular dynamic simulation of the dock complex of VLL-28 with CatL using GROMACS.

Results: We observed a strong interaction of VLL-28 with CatL, and a molecular dynamic simulation study further confirmed a stable interaction between VLL-28 and CatL.

Discussion: Difficulties in treatment mode and for efficiently treating conditions stand out, making anti-cancer peptide therapies a viable next-generation treatment. Peptide binding dynamics and affinity to CatL are highlighted in the investigation, especially in light of the development of innovative therapeutic approaches for the treatment of cancer.

Conclusion: Our study suggests VLL-28 peptide may be a good therapeutic candidate for EOC as a CatL inhibitor. Although, further wet lab validations are suggested.

Keywords: Anticancer Peptide, Cancer, Ovarian Cancer, In-silico, Molecular Docking, Molecular Dynamic Simulation.

How to cite this article: Choudhary A, Kumari N, Sharma PK, Shrivastava SK, Niraj RRK, Sharma V, Computational Study of the Anti-cancer Peptide VLL-28 Targeting Cathepsin L to Combat Epithelial Ovarian Cancer. Int J Drug Deliv Technol. 2026;16(5): 323-332. DOI: 10.25258/ijddt.16.5.34

Source of support: Nil.

Conflict of interest: None

1. INTRODUCTION

Ovarian cancer (OC) is the seventh most common cause of death and morbidity globally and is regarded as one of the deadliest gynecologic cancers (Modugno & Edwards, 2012). The fact that OC is frequently asymptomatic and that roughly two-thirds of patients are not diagnosed until the disease has progressed to stages III or IV. In industrialized nations, ovarian cancer is the second most common cancer among women aged 40 and older, following breast cancer [1].

There are three main types of ovarian cancer: sex cord-stromal tumors (which account for only about 5% of all ovarian malignancies), germ cell tumors, and epithelial tumors—the latter being the most common. Ovarian cancer is associated with numerous risk factors and typically affects postmenopausal women, with its incidence, progression, and survival rate increasing with age [2]. Unlike other tumors, ovarian cancer generally remains asymptomatic until it reaches an advanced stage, often leading to delayed diagnosis and a poor prognosis. Currently, there are no well-structured preventive programs in place for OC. The disease has a high recurrence rate and mortality, largely due to genetic mutations—such as BRCA mutations and homologous recombination deficiency (HRD)—that are linked to a high incidence of OC.

**Author for Correspondence: vinaysharma30@yahoo.co.uk*

Surveillance and preventive treatment programs are typically available only for high-risk women [3]. The World Health Organization estimates that ovarian cancer will be diagnosed in 225,500 cases per year, with approximately 140,200 deaths resulting from the disease. This makes ovarian cancer the seventh most prevalent kind of cancer and the eighth most common cause of cancer-related death for women globally [4, 5]. When combined, these numbers highlight the importance of ovarian cancer as a cause of illness and death for people worldwide. Ovarian cancer ranks fifth among women in Western countries who die from cancer [6]. The Surveillance, Epidemiology, and End Results (SEER) program of the American National Cancer Institute (NCI) reports that there are 10.2 new cases of ovarian cancer per 100,000 women annually. The annual death rate is 6.0 per 100,000 women. These age-adjusted rates are based on incidence data from 2017 to 2021 and mortality data from 2018 to 2022. In 2021, an estimated 238,484 women were living with ovarian cancer (SEER Ovarian Cancer). The 5-year overall survival from ovarian cancer has remained almost stable since roughly 1980, according to a recent meta-analysis that drew upon survival data from several nations, despite notable improvements in the previous 50 years in the survival rates for certain solid tumors [7]. The most recent data from the SEER (2014–2020) indicates that the US's 5-year survival rate is now about 50.9% (SEER Ovarian Cancer). The most common cause of mortality from gynecologic cancers is epithelial ovarian cancer (EOC), which has a poor prognosis because of its generally vague early symptoms, which frequently indicate an advanced stage of metastasized disease at presentation [8]. EOC mostly spreads by the transcoelomic pathway, allowing exfoliated tumor cells to spread throughout the abdominal cavity and especially to the omentum. One cysteine protease that may be used as a therapeutic target in the treatment of cancer is cathepsin L. Cancer progression may be slowed by inhibiting the activity of particular proteases. There is uncertainty regarding the impact of cathepsin L inhibition alone on angiogenesis and apoptosis in cancer. Although targeted suppression of cathepsin L appears to decrease invasion and metastasis, there is concern that this may cause other cathepsins to compensate. Inhibiting cathepsin L in conjunction with traditional chemotherapy appears to be more promising and has produced more reliable outcomes. Cell surface expression of cathepsins allows them to be released into the extracellular environment, where they can break down extracellular matrix components. Cathepsins exhibit their proteolytic action when they bind to other cell surface proteins. Because of this extracellular activity, cancer cells can spread to other locations by invading nearby tissues, blood vessels, and lymphatic vessels. Cathepsins are therefore thought to be attractive targets for anticancer treatment [9]. Using in-silico techniques of molecular modeling, molecular docking, and molecular dynamic simulation study, this work focuses on the selection, design, and screening of anticancer peptides as well as examining their patterns of interaction with a particular protein.

2. MATERIALS AND METHOD

2.1 Target Selection

The study focuses on studying the CatL target protein of EOC. The RCSB Protein Data Bank website (https://www.rcsb.org) provided the crystallographic structural details of the CatL protein for this purpose. The target protein's PDB ID is 4AXL.

2.1.1 Target protein binding pocket prediction

The Computer Atlas of Surface Topography of Proteins (CASTp) server was utilized to predict the active binding site (http://sts.bioe.uic.edu/castp/index.html?2cpk). A flexible tool called CASTp was created to reveal the complex surface characteristics and essential functional areas of proteins. By facilitating the identification, visualization, and quantification of concave surface regions within protein structures, it empowers researchers in predicting crucial binding pockets and cavities embedded within protein surfaces [10]. The predicted active binding sites were verified using the PeptiMap server (https://peptimap.cluspro.org), guaranteeing their precision and dependability. This server pinpoints the precise location where peptides bind within protein complexes, ranking these predictions at the top for the majority of cases in a meticulously curated dataset of high-quality structures [11].

2.1.1 Subcellular localization prediction

CELLO V.2.2 was used to predict subcellular localization (http://cello.life.nctu.edu.tw). The multi-class Support Vector Machines classification system is the method that depends on it. One-against-one (OAO) classification is utilized for multi-class SVMs. 5*(5-1)/2=10 SVM classifiers are built for each of the five classes of subcellular locations, and each classifier is proficient when working with proteins from two different subcellular locations. Cross-validation in conjunction with the one-against-one (1A1) method is used for each kernel and penalty parameter to assess the model's execution.

2.2 Selection of ligands

The database of antimicrobial peptides (https://aps.unmc.edu) contains about 3940 AMPs. More than 3146 naturally occurring AMPs with verified antimicrobial activity were listed as of January 2024. To meet the database's rigorous standards, peptides must fulfill specific criteria: they must originate from natural sources spanning three domains or six kingdoms, demonstrate antimicrobial efficacy (with a minimum inhibitory concentration of less than 100 μM or 100 μg/mL), have their mature amino acid sequences at least partially elucidated, and contain fewer than 100 amino acid residues [12, 13]. From this APD database, 274 ACPs were retrieved for further study.

2.2.1. Physicochemical characteristics of the chosen anticancer peptide:

The ProtParam server was utilized to evaluate the physicochemical characteristics of the chosen anticancer peptide (https://web.expasy.org/protparam/). Mass, predicted isoelectric point (pI), net charge, extinction coefficient and hydrophobicity, instability index, aliphatic index, grand average of hydropathicity (GRAVY), and estimated half-life are all included in the computed parameters. Along with these descriptors, other features were also explored using in-silico tools like the ToxinPred server (http://crdd.osdd.net/raghava/toxinpred/), which is used to calculate the toxicity [14], and the PeptideRanker (http://distilldeep.ucd.ie/PeptideRanker/) tool was employed to examine bioactivity, and water solubility was assessed using the Innovagen server (http://www.innovagen.com) tool [15].

2.2.2 Peptide sequence structural prediction:

The PepDraw server (https://www2.tulane.edu/~biochem/WW/PepDraw/) was used to predict the peptide sequence's primary structure. Protein structures can be accurately predicted thanks to deep neural networks like AlphaFold2. This tool is an indispensable asset for precisely predicting the tertiary structure of anticancer peptides [16].

2.3 Preparing the target and ligand for molecular docking

UCSF Chimera (https://www.cgl.ucsf.edu/chimera/) was used to optimize and minimize the energy of structures. It is effective in eliminating all non-standard residues, removing ligand structures that are already present in the target protein, and altering a number of other parameters, including the addition or removal of charges, water molecules, or any other specific amino acid.

2.4 Molecular docking

Docking of the CatL target protein with the anti-cancer peptides was performed using the HDOCK server (http://hdock.phys.hust.edu.cn) [17]. This user-friendly server combines template-based modeling, homology search, and job management for quick and reliable protein-protein docking, macromolecular docking, and structure prediction. The hybrid algorithm of template-based and template-free docking makes the prediction automatically.

2.5 Molecular Dynamics Simulation

The GROMACS 2020 package (ftp://ftp.gromacs.org/pub/gromacs/gromacs-2020.tar.gz) was used to perform the MD simulation. The default water model was chosen for the simulation, and the Charmm 36 (charmm36-jul2021.ff.tgz) was used as a force field for the process. The steps were prompted by the preparation of protein topology and the ligand topology, followed by the energy minimization steps. The equilibration of the system was done by the NVT and NPT. The final production of the molecular dynamics was 100 ns. Analysis of the MD simulation incorporates the graph of RMSD (Root-Mean-Square Deviation), RMSF (Root-Mean-Square Fluctuation), and residue of gyration [18, 19, 20].

3. RESULT AND DISCUSSION

A promising and economical method that is essential to the drug discovery and development pipeline is the identification of drug candidates through computational screening [21]. Medicinal chemists can better cover the wide range of theoretical aspects of contemporary drug development by using computational chemistry-based methodologies in target identification and drug discovery [22].

3.1 CatL EOC Target Protein:

The CatL target protein's crystallographic structure information was obtained from the RCSB website for a protein data bank. 4AXL is the protein's PDB ID.

3.1.1 Target protein binding pocket prediction

The CASTp server's prediction of the binding pocket revealed a total of 29 pockets. Three pockets had the largest surface area among them. According to Figure 1, the biggest pocket is 167.113 in volume and roughly 218.636 in surface area.

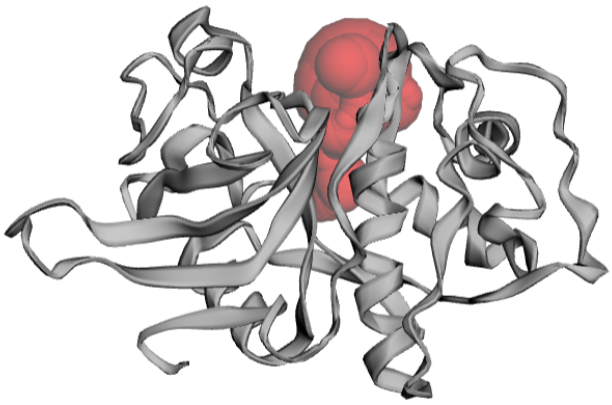

Figure 1. Prediction of active binding pockets of CatL target protein of EOC using CASTp server.

The anticipated active site Using the PeptiMap server, Chain A of the CatL target protein displayed the three prominent locations listed in Table 1.

Table 1. Active binding site prediction of the target protein CatL of the EOC through the PeptiMap Server.

S.No.	Active binding sites	Residues present on the active binding site of CatL protein
1.	Site 1	ASN A 18,GLN A 19,GLY A 20,GLN A 21,CYS A 22,GLY A 23,SER A 24,CYS A 25,TRP A 26,GLY A 67,GLY A 68,LEU A 69,MET A 70,ALA A 135,ILE A 136,ALA A 138,GLY A 139,HIS A 140,PHE A 143,LEU A 144,MET A 161,ASP A 162,HIS A 163,GLY A 164,SER A 188,TRP A 189,GLY A 190
2.	Site 2	LEU A 69,MET A 70,ASP A 71,ASP A 114,SER A 133,ALA A 214,ALA A 215,SER A 216
3.	Site 3	ARG A 8,VAL A 13,THR A 14,PRO A 15, VAL A 16,LYS A 186,GLU A 191,GLY A 196,TYR A 198

3.1.2 Subcellular localization prediction:

CELLO v.2.5 predicts that the target protein is found in the cytoplasm by identifying the protein's subcellular location within the cell.

3.2. Ligand Selection:

274 anticancer peptides were obtained from the online Antimicrobial Peptide Database (APD3) (https://aps.unmc.edu/home) in order to target the EOC CatL. In order to reach the target, 274 different peptide sequences were investigated. Physiochemical characteristics were the basis for the choice. Among these peptide sequences, VLL-28 (APD-ID: AP03049) was identified as a possible medication candidate that might be used to treat EOC.

3.2.1 Potential drug candidates' physicochemical characteristics:

The VLL-28 descriptors are listed in Table 2. According to the table, VLL-28's peptide sequence has better stability than others. For this reason, the anticancer peptide VLL-28 (APD ID: AP03049) was selected to investigate its molecular interaction with the EOC target CatL protein. Table 3 displays the specific characteristics of the VLL-28.

Table 2. Potential drug candidates with their physio-chemical properties:

S.no.	Features	VLL-28
1.	APD-ID	AP03049
2.	Instability Index	Stable (-5.33)
3.	Toxicity	Non-toxic
4.	Estimated half-life (Mammalian reticulocyte, in vitro)	100 hours
5.	Allergenicity	Probable non-allergen
6.	Bioactivity	0.585676
7.	Water solubility	Good

Table 3. Physicochemical attributes of anticancer peptide VLL-28 anticipated through Antimicrobial Peptide Database, PepDraw server, Peptide Ranker, Innovagen server and AllergenFP server.

S.No.	Attributes	Antimicrobial Peptide (VLL-28)
1	Peptide Sequence	VLLVTLTRLHQRGVIYRKWRHFSGRK YR
2	Source	*Sulfolobus islandicus*
3	Length	28
4	Net charge	9
5	Mass	3540.67
6	Isoelectric point (pI)	12.02
7	Hydrophobicity	-0.05 Kcal * mol -1
8	Instability Index	Stable (-5.33)
9	Extinction coefficient (mammalian reticulocyte, in vitro)	100 hours
10	Water solubility	Good
11	Bioactivity	0.585676
12	Aliphatic Index	100.71
13	Grand average of hydropathicity (GRAVY)	- 0.575
14	Hydrophobic residues %	35%
15	Boman Index	2.87

16	Toxicity	Non-toxic
17	Activity	Anti-Gram+ & Gram-, Antifungal, candidacidal, Antibiofilm, Anticancer

3.2.2 Anticancer Peptide's Structural Prediction:
Using the PepDraw server, the peptide VLL-28's primary structure prediction is predicted and shown in Figure 2. The AlphaFold2 server is used to predict the tertiary structure of the peptide VLL-28, as seen in Figure 3. Because AlphaFold2 uses a deep learning algorithm, the results are accurate. Consequently, the AlphaFold2 server produces five models, and the model with the highest score, ranked 1, was chosen.

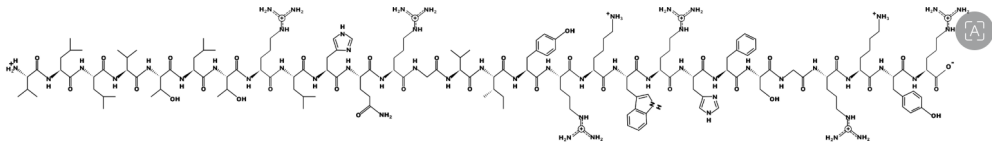

Figure 2. Primary structure prediction of anticancer peptide VLL-28 through the PepDraw server.

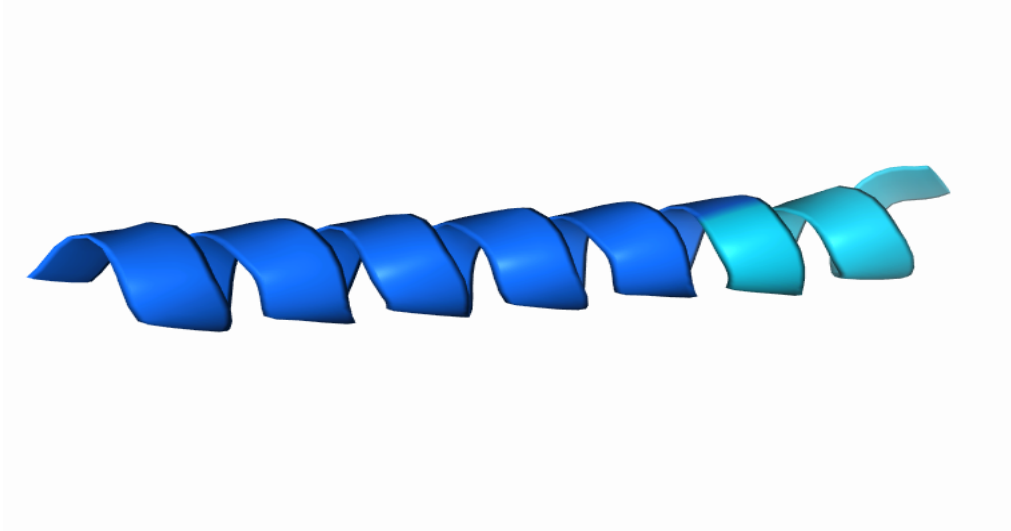

Figure 3. Structure prediction of anticancer peptide VLL-28 through the Alphafold server

3.3 Target and ligand molecule preparation:
Chimera software was used to prepare the ligand and receptor molecules for molecular docking. All contaminants and unnecessary components were carefully removed prior to the docking step.

3.4 Molecular Docking:
Using the HDOCK server, the target protein CatL (PDB ID: 4AXL) was docked with the chosen anticancer peptide. Table 4 displays the output file that the HDOCK server produced. Model 8 of the docked model complex was selected because it demonstrated a binding score of -233.04 kcal/mol and successfully bound to the target protein's active binding site. The HDOCK server calculates the confidence score based on the docking score; for molecules to be more likely to bind together, the score must be greater than 0.7. The confidence score for this model complex of the peptide VLL-28 and the target protein CatL is 0.8403. Figures 4(a) and 4(b) show the molecular docking of the model complex CatL-VLL 28. Docking interaction also shows protein-peptide molecular interaction between the target protein CatL and the VLL-28 peptide shown in Table 5.

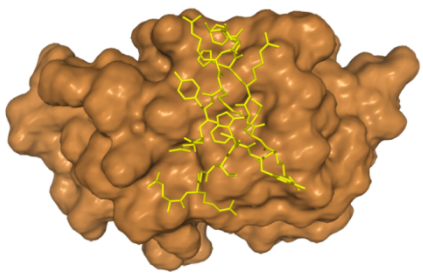

(a)

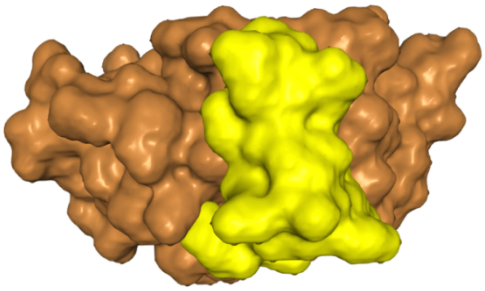

(b)

Figure 4. The docked model complex of CatL target protein (4AXL) and anticancer peptide VLL-28 anticipated using HDOCK server. Figure **4(a)** shows model 8 (in Yellow) of the ligand VLL-28 in licorice form and Figure **4 (b)** shows the ligand in the surface form.

Table 5. Protein-peptide molecular interaction between the target protein CatL and the VLL-28 peptide:

S.no.	Interaction of amino acid residues present on the active bind site of the model complex (CatL-VLL-28)	Distance (Å)
1.	(GLU) 87A - (TYR)9A	2.575
2.	(ARG)91A - (VAL)6A	3.160
3.	(ARG)91A - (GLY)8A	3.596
4.	(LYS)92A - (VAL)6A	4.811
5.	(LYS)140A - (TYR)5A	4.117
6.	(ASP)141A - (TRP)3A	4.774
7.	(ASP)141A - (TRP)16A	4.660
8.	(TYR)142A - (TRP)3A	3.995
9.	(TYR)142A - (TYR)5A	2.732
10.	(TYR)142A - (PHE)7A	3.290
11.	(TYR)142A - (TRP)16A	4.374
12.	(HIS)145A - (TRP)3A	3.321
13.	(HIS)145A - (TYR)5A	4.467
14.	(HIS)145A - (TRP)16A	2.643
15.	(PRO)146A - (TYR)5A	5.000
16.	(PRO)146A - (ALA)14A	3.827
17.	(LYS)147A - (TYR)5A	2.743
18.	(LYS)147A - (VAL)6A	4.773
19.	(LYS)147A - (PHE)7A	2.161
20.	(LYS)147A - (ASN)12A	3.118
21.	(LYS)147A - (ALA)14A	3.830
22.	(GLU)148A - (ASN)12A	2.910
23.	(GLU)148A - (CYS)13A	2.869
24.	(GLU)148A - (ALA)14A	3.680
25.	(ASN)149A - (ASN)12A	3.415
26.	(TYR)151A - (PHE)7A	4.191
27.	(HIS)155A - (PHE)7A	2.825
28.	(ARG)193A - (PHE)7A	3.047
29.	(ARG)193A - (GLY)8A	4.540
30.	(ARG)193A - (TYR)9A	3.564
31.	(ARG)193A - (GLY)10A	3.592
32.	(TYR)194A - (PHE)7A	4.630
33.	(TYR)194A - (GLY)8A	3.551
34.	(TYR)194A - (TYR)9A	3.227

3.5 Molecular Dynamics Simulation:

GROMACS was used to evaluate the MD simulation results for about 100 ns. The root-mean-square deviation (RMSD) of protein Cα atoms bound to the peptide is represented graphically in Figure 5(a), where the RMSD was calculated using the initial equilibrated structure as a reference. Early in the simulation, the RMSD rapidly increases from 0 to about 0.2 nm, indicating early structural changes of the protein-peptide complex.

Following the initial rise, the RMSD gradually increases and varies between 0.2 and 0.6 nm, indicating that the complex is still undergoing conformational changes and flexibility. The RMSD values tend to stabilize and oscillate around 0.6 nm after 75 ns, which might suggest that the system is approaching a relatively stable conformational state. Beyond the 0.6 nm threshold, there are no appreciable increases or decreases in RMSD, indicating that the protein-peptide complex is not undergoing any significant disruptions or extensive structural alterations. The root-mean-square fluctuation (RMSF) of protein residues bound to peptides is shown in Figure 5(b). The RMSF values are typically low (below 0.1-0.2 nm), with only a sharp pickup to 0.4 nm seen at residue 100. This suggests that the protein's interior regions are comparatively stable and undergo little fluctuation when bound to the peptide. Nearly all residues show slight variations, suggesting that the protein's core is stable. The interaction between the protein and the peptide may depend on this stability. The radius of gyration of the protein in its bound state with the peptide after 100 ns of simulation is shown in Figure 5(c). The Rg values vary between roughly 1.69 and 1.71 nm during the simulation, indicating continuous conformational changes and dynamic behavior of the protein-peptide complex.

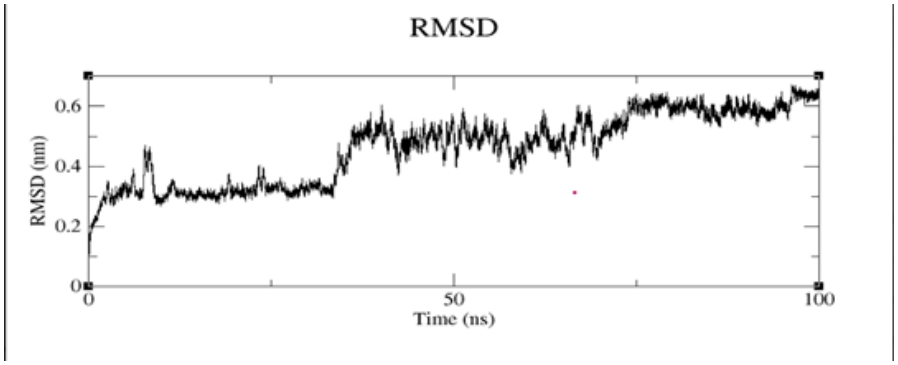

(a)

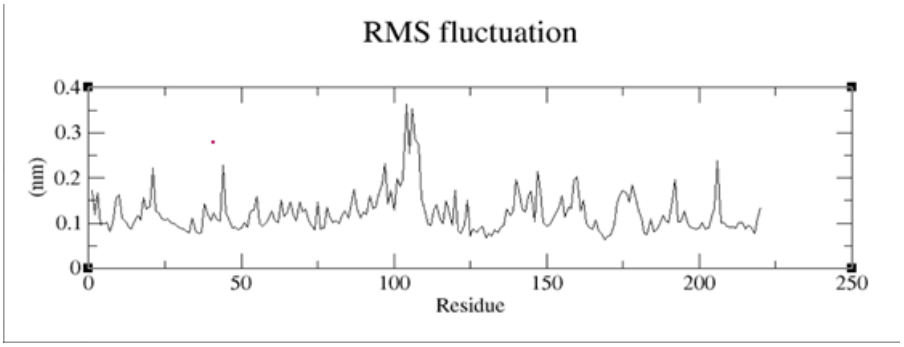

(b)

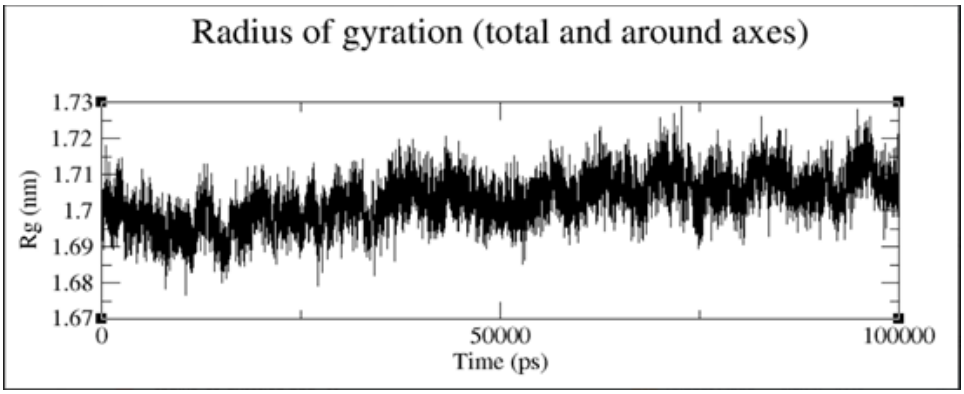

(c)

Figure 5. MD simulation of the protein-peptide model complex CatL protein (4AXL) and VLL-28 for 100 ns: **(a)** Root-mean-square deviation, **(b)** Root-mean-square fluctuation, **(c)** Radius of gyration

Figure 6 displays the average solvent accessible surface area (SASA) of each protein residue when it is attached to a peptide. Throughout the simulation, the SASA values fluctuate between 0 and 2 nm², with an average value of about 0.5 nm². This indicates dynamic changes in the protein's conformation and its interaction with the solvent. The protein appears to maintain a comparatively constant solvent-exposed surface area throughout the simulation, as evidenced by the lack of notable jumps or drops in SASA. Figure 7 depicts the hydrogen bonds that developed between the protein and peptide during the 100 ns simulation.

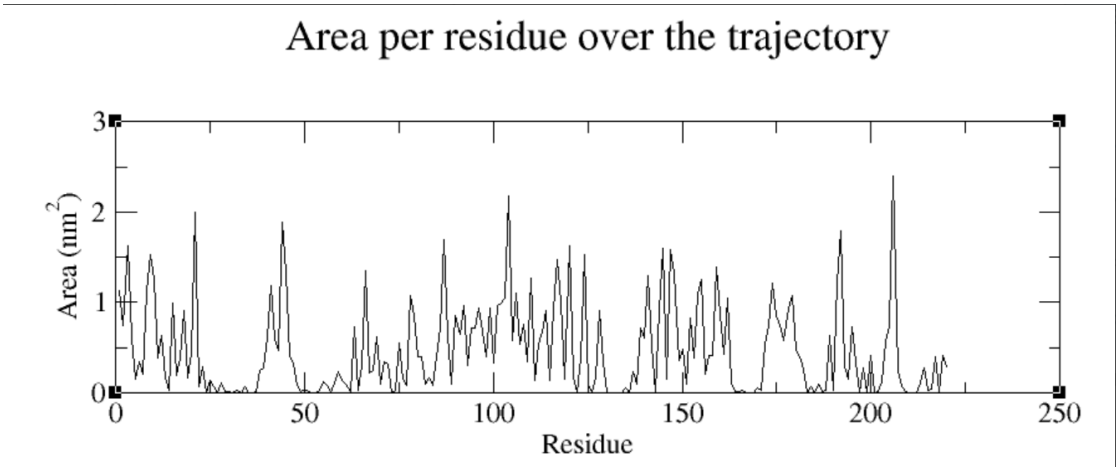

Figure 6: Graphical representation of Solvent accessible surface area for assessing the protein-peptide interaction.

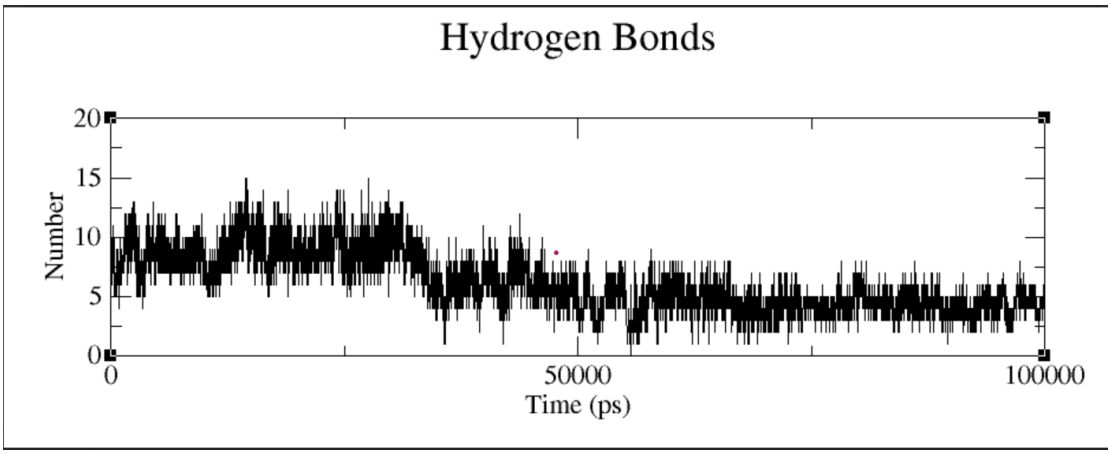

Figure 7. Hydrogen bonds formed between protein and peptide during 100 ns of simulation.

4. CONCLUSION

There are several computer frameworks available for in-silico therapeutic molecule repurposing [23]. The acknowledged advantages of repurposing in assisting with new drug research initiatives, as well as the growing desire to include clinical data in regulatory approval procedures, have led to the development of molecules. A promising and economical method essential to the drug discovery and development pipeline is the identification of drug candidates through computational screening, which encompasses a wide range of theoretical aspects of contemporary drug development by utilizing computational chemistry-based methodologies in target identification and drug discovery. Our study will provide good insight into peptide therapeutics for EOC. With a binding score of -233.04 kcal/mol, the peptide successfully attaches to the target protein CatL's active binding site. The server produced a confidence score of 0.8403 based on the docking score. Further MD simulations were evaluated for around 100 ns using GROMACS software. This study reports the VLL28 peptide as a potent peptide inhibitor of target protein 4AXL (CatL). This peptide may work as a peptide therapeutics option for the treatment of EOC after critical validation and improvisation in in vitro experiments. This approach will aid the future search and development of novel anticancer peptides for targeting EOC by expanding the utilization of biological resources. To confirm or further determine the strength of these interactions and the stoichiometry of the protein-peptide interaction, a number of in vitro and in vivo studies will undoubtedly need to be conducted. This will provide additional information for the design and development of a new or alternative treatment regimen for EOC.

Limitations of study: We suggest further validation of the outcome of our study in in-vitro and in-vivo studies.

Figure Caption:

Figure 1. Prediction of active binding pockets of CatL target protein of EOC by CASTp.

Figure 2. Primary structure prediction of anticancer peptide VLL-28 through the PepDraw server.

Figure 3. Structure prediction of anticancer peptide VLL-28 through the Alphafold server

Figure 4. The docked model complex of CatL target protein (4AXL) and anticancer peptide VLL-28 anticipated using HDOCK server. Figure **4(a)** shows model 8 (in Yellow) of the ligand VLL-28 in licorice form and Figure **4 (b)** shows the ligand in the surface form.

Figure 5. MD simulation of the protein-peptide model complex CatL protein (4AXL) and VLL-28 for 100 ns: **(a)** Root-mean-square deviation, **(b)** Root-mean-square fluctuation, **(c)** Radius of gyration

Figure 6: Graphical representation of Solvent accessible surface area for assessing the protein-peptide interaction.

Figure 7. Hydrogen bonds formed between protein and peptide during 100 ns of simulation.

Author contributions

The authors confirm their contribution to the paper as follows: Study conception and design: VS and RRKN; data collection: AC; Data Analysis or Interpretation: AC, SKS, NK, PKS and RRKN; methodology: AC: investigation: AC; draft manuscript: AC. All authors reviewed the results and approved the final version of the manuscript.

Abbreviations:

EOC- Epithelial Ovarian Cancer; CatL- Cathepsin L; OC-Ovarian Cancer; HRD-Homologous recombination deficiency; SEER -Surveillance, Epidemiology, and End Results; CASTp - Computer Atlas of Surface Topography of Proteins; SVM classification- Support Vector Machines classification; AMPs- Antimicrobial Peptides; ACPs-Anticancer Peptides; ADP Database antimicrobial peptide database.

ETHIC APPROVAL AND CONSENT TO PARTICIPATE

Not applicable.

HUMAN AND ANIMAL RIGHTS

Not Applicable.

CONSENT FOR PUBLICATION

Not applicable.

AVAILABILITY OF DATA AND MATERIAL

All data generated or analyzed during this study are included in this published article.

FUNDING

None.

CONFLICT OF INTEREST

The author(s) declare no conflict of interest, financial or otherwise.

ACKNOWLEDGEMENTS

The author acknowledges Amity Institute of Biotechnology, Amity University Rajasthan, Jaipur, Rajasthan, India for providing infrastructure facilities.

REFERENCES

1. Zheng M, Li X, Hu Y, Dong H, Gou R, Nie X, Liu Q, Ying-Ying H, Liu J and Lin B. (2019). Identification of molecular marker associated with ovarian cancer prognosis using bioinformatics analysis and experiments. *Journal of Cellular Physiology*. **234**(7) pp 11023–11036. Doi: https://doi.org/10.1002/jcp.27926.

2. Okwuosa T. M, Morgans A, Rhee J-W, Reding K. W, Maliski S, Plana J.-C, Volgman A. S, Moseley K. F, Porter C. B and Ismail-Khan R. (2021). Impact of Hormonal Therapies for Treatment of Hormone-Dependent Cancers (Breast and Prostate) on the Cardiovascular System: Effects and Modifications: A Scientific Statement From the American Heart Association. Circulation. *Genomic and Precision Medicine* **14**(3) pp e000082. Doi: https://doi.org/10.1161/HCG.0000000000000082

3. Dochez, V., Caillon, H., Vaucel, E., Dimet, J., Winer, N., and Ducarme, G. (2019). Biomarkers and algorithms for diagnosis of ovarian cancer: CA125, HE4, RMI and ROMA, a review. *Journal of Ovarian Research*. **12**(1) p. 28. doi: https://doi.org/10.1186/s13048-019-0503-7

4. Jemal A, Bray F, Center M.M, Ferlay J, Ward E and Forman D.(2011). Global cancer statistics. *CA Cancer J. Clin*.**61**:pp 69–90. Doi: **https://doi.org/10.3322/caac.20107**

5. Ferlay J., Soerjomataram I., Dikshit R., Eser S., Mathers C., Rebelo M., Parkin D.M., Forman D and Bray F. (2012). Cancer incidence and mortality worldwide: Sources, methods and major patterns in GLOBOCAN. *Int. J. Cancer*. **136** ppE359–E386. Doi: **https://doi.org/10.1002/ijc.29210**

6. Berns E.M and Bowtell D.D. (2012). The changing view of high-grade serous ovarian cancer. *Cancer Res.* **72** pp 2701–2704.doi: https://doi.org/10.1158/0008-5472.CAN-11-3911

7. Vaughan S, Coward J.I, Bast R.C, Berchuck A, Berek J.S, Brenton J.D, Coukos G, Crum C.C. and Drapkin R. Etemadmoghadam, D. (2011). Rethinking ovarian cancer: Recommendations for improving outcomes. *Nat. Rev. Cancer*. **11**: pp 719–725. Doi:https://www.nature.com/articles/nrc3144

8. Md Zahidul Islam Pranjol, Nicholas Gutowski, Michael Hannemann and Jacqueline Whatmore. (2015). The Potential Role of the Proteases Cathepsin D and Cathepsin L in the Progression and Metastasis

of Epithelial Ovarian Cancer. *Biomolecules*.**5**: pp:3260-3279 doi:https://doi.org/10.3390/biom5043260

9. Gocheva V, Joyce JA. Cysteine cathepsins and the cutting edge of cancer invasion. Cell Cycle. 2007 Jan 1;6(1):60-4. doi: 10.4161/cc.6.1.3669. Epub 2007 Jan 6. PMID: 17245112.
10. Binkowski, T. A. CASTp: Computed Atlas of Surface Topography of Proteins. *Nucleic Acids Research* **2003**, *31* (13), 3352–3355. https://doi.org/10.1093/nar/gkg512.
11. Lavi, A.; Ngan, C. H.; Movshovitz-Attias, D.; Bohnuud, T.; Yueh, C.; Beglov, D.; Schueler-Furman, O.; Kozakov, D. Detection of Peptide-Binding Sites on Protein Surfaces: The First Step toward the Modeling and Targeting of Peptide-Mediated Interactions. *Proteins: Structure, Function, and Bioinformatics* **2013**, *81* (12), 2096–2105. https://doi.org/10.1002/prot.24422.
12. Wang, Z. APD: The Antimicrobial Peptide Database. *Nucleic Acids Research* **2004**, *32* (90001), 590D592. https://doi.org/10.1093/nar/gkh025.
13. Wang, G.; Li, X.; Wang, Z. APD3: The Antimicrobial Peptide Database as a Tool for Research and Education. *Nucleic Acids Research* **2015**, *44* (D1), D1087–D1093. https://doi.org/10.1093/nar/gkv1278.
14. Gupta, S.; Kapoor, P.; Chaudhary, K.; Gautam, A.; Kumar, R.; Raghava, G. P. S. In Silico Approach for Predicting Toxicity of Peptides and Proteins. *PLoS ONE* **2013**, *8* (9), e73957. https://doi.org/10.1371/journal.pone.0073957.
15. Dimitrov, I.; Naneva, L.; Doytchinova, I.; Bangov, I. AllergenFP: Allergenicity Prediction by Descriptor Fingerprints. *Bioinformatics* **2013**, *30* (6), 846–851. https://doi.org/10.1093/bioinformatics/btt619.
16. Tomer Tsaban; Varga, J.; Orly Avraham; Ziv Ben-Aharon; Khramushin, A.; Schueler-Furman, O. Harnessing Protein Folding Neural Networks for Peptide–Protein Docking. **2022**, *13* (1). https://doi.org/10.1038/s41467-021-27838-9.
17. Yan, Y.; Zhang, D.; Zhou, P.; Li, B.; Huang, S.-Y. HDOCK: A Web Server for Protein–Protein and Protein–DNA/RNA Docking Based on a Hybrid Strategy. *Nucleic Acids Research* **2017**, *45* (W1), W365–W373. https://doi.org/10.1093/nar/gkx407.
18. Huang, J.; MacKerell, A.D. CHARMM36 All-Atom Additive Protein Force Field: Validation Based on Comparison to NMR Data. *J. Comput. Chem.* **2013**, *34*, 2135–2145, doi:10.1002/jcc.23354.
19. Bauer, P.; Hess, B.; Lindahl, E. GROMACS 2022.4 Manual. **2022**, doi:10.5281/ZENODO.7323409.
20. Darden, T.; York, D.; Pedersen, L. Particle Mesh Ewald: An $N \cdot \log(N)$ Method for Ewald Sums in Large Systems. *J. Chem. Phys.* **1993**, *98*, 10089–10092, doi:10.1063/1.464397.
21. Brogi, S.; Ramalho, T. C.; Kuca, K.; Medina-Franco, J. L.; Valko, M. Editorial: In Silico Methods for Drug Design and Discovery. Front. Chem. 2020, 8, 612, DOI: 10.3389/FCHEM.2020.00612
22. Ou-Yang, S. S.; Lu, J. Y.; Kong, X. Q.; Liang, Z. J.; Luo, C.; Jiang, H. Computational Drug Discovery. Acta Pharmacol. Sin. 2012, 33, 1131– 1140, DOI: 10.1038/aps.2012.109
23. Mullins, J. G. L. Drug Repurposing *in Silico* Screening Platforms. *Biochemical Society Transactions* **2022**, *50* (2), 747–758. https://doi.org/10.1042/bst20200967.